GEM TN-93-283
MIT-GEM-EM-15

Joule Heating of GEM Detector Radiation Shields

A. Radovinsky
Plasma Fusion Center, Massachusetts Institute of Technology

January 27, 1993

Abstract:

Studies were carried out to determine Joule heating in and Lorentz forces acting on the GEM detector magnet LN radiation shields using the program EDDYCUFF. The effects seen during coil charge and discharge have been compared. Panels with various cooling tube configurations have been analyzed. Configurations include: electrically interconnected tubes of adjoining panels; panels with tubes having electrical insulating breaks; and panels with no tubes. The distributions of the heating energy and of the electromagnetic forces between the outer, inner and end panels of the radiation shields were obtained. In addition the effects related to the superinsulation have been analyzed.

MIT-GEM-EM-15

Joule Heating of GEM Detector Radiation Shields

27 January 1993

A. Radovinsky

This document and all reports and memoranda in this series are intended as a record of work in progress. They are for use in informal discussions of design and fabrication alternatives. This material is subject to change and should not, therefore, be published or referred to in the open literature. Conclusions are preliminary and distribution should be strictly limited.

Plasma Fusion Center
Massachusetts Institute of Technology
Cambridge, MA 02139

MIT GEM Detector Memoranda
Approval Sheet

B.A. Smith
Project Engineer

1/28/93
Date

R.D. Pillsbury, Jr.
Technical Monitor

1/25/93
Date

A.M. Dawson
Technical Editor

26 Jan 93
Date

Abstract

Studies were carried out to determine Joule heating in and Lorentz forces acting on the GEM detector magnet radiation shields. The effects seen during coil charge and discharge have been compared. Panels with various cooling tube configurations have been analyzed. Configurations include: electrically interconnected tubes of adjoining panels; panels with tubes having electrical insulating breaks; and panels with no tubes. The distributions of the heating energy and of the electromagnetic forces between the outer, inner and end panels of the radiation shields were obtained. In addition the effects related to the superinsulation have been analyzed.

The Model

The program EDDYCUFF[1] was used in these analyses. EDDYCUFF assumes that the conducting medium is a shell which is thin relative to the skin depth, which implies a uniform distribution of current density through its thickness. This also implies that there is no current flow perpendicular to the plane of the shell. The dimensions of the model are shown in Fig.1. An axial cross section of a set of 12 cylindrical coil modules, thin conducting bobbins, and radiation shields are shown with axial symmetry about the Z-axis and a plane of symmetry at Z=0. An axial view of the panels is given in the box in Fig.1. There are 16 such panels in each shield.

The coils were modeled as uniform current density solenoids with a centroidal radius of 9.5 m, thickness of 0.02 m, and length in the Z-direction of 0.9709 m. The current (I) in each solenoid is the same. The effects of the magnetic fields due to the eddy currents induced in the elements of the bobbins (such as bobbin walls, radiation intercepts, etc.) were not taken into account, since it was shown that their values did not exceed 1% of the driving fields of the solenoids.

The panels were modeled as cylindrical shells with centroidal radii of 9.202 and 10.024 m for the inner and outer shields respectively. A thickness of 0.00318 m, length in Z-direction of 14.60 m, and resistivity of $1.65*10^{-8}$ ohm*m (Al 6061 at 77 K)[2] were used. Figure 2 shows the mesh in a half panel. Since shields were considered together with the tubes (laid along line ABCD on Fig. 2), an additional thickness, equivalent to the cross section of a tube (0.00102 m^2) was added to the thickness of the elements along the line ABCD and the resistivity of these elements was changed to $3.50*10^{-9}$ ohm*m (Al 1100 at 77 K)[2]. The edges of the panels are electrically insulated from each other. The tubes of adjoining panels are electrically connected (at point A of Fig. 2), so all 16 panels of each shield are resistively shorted in the circumferential direction. The arc length (2*AB) of the tube interconnecting adjacent panels is one half the arc length of a single panel.

The end panels (see Fig.1) located in between the cylindrical shells at Z=0.575 m (referred to in what follows as the left end panel) and at Z=15.175 m (right end panel) are modeled as 16 insulated segments of an annulus with the same thickness and resistivity as those of the cylindrical panels.

Comparison of Charge and Discharge

Two regimes were considered. They were:

* Charging the coils with a linear current ramp from 0 to 950 kA for 8 hours;

* Discharge with an exponential current decay with a time constant of 100 s. That is

$$I=950*\exp(-t/100) \quad kA$$

The results of the study are summarized in Table 1. The table shows the values of the thermal energy (in joules) and the maximum values of the power (in watts) generated in all 16 panels of each of the shields. Also listed in Table 1 are the components of the electromagnetic force that acts on one panel half corresponding to Y>0 in the coordinates shown in the box in Fig.1 and in Fig. 2. The values of the power and the forces are uniform during charge, while during discharge they decay exponentially after a peak at 1 second.

Table 1 shows that the total energy generated during discharge is more than 140 times higher than that generated during charge. A maximum of less than 0.7 MJ is deposited in either all of the inner or all of the outer shields during discharge.

The peak values of the power of Joule losses at the beginning of discharge are substantially larger (by 10^5) than during the charge. A maximum of about 13 kW is deposited in each of the shields (made up of 16 panels) during discharge.

Since the analyses were carried out with the assumption that the panels are rigid bodies, only the components of the total forces acting on a panel half have been calculated without specifying the points of their application. Table 1 shows that the forces do not exceed 8 kN. Maximum values of Fx and Fy (which if negative might buckle the panel) are positive; the only case (charge of the inner shield) with negative Fx and Fy (which is the worst for stability) shows very small forces.

As is shown by the data in Table 1, the heating and the forces during discharge are much higher than during charge. Therefore, only discharge is considered further.

Comparative Design of the Panels

Some modifications of the model were considered. Table 2 presents the power, energy and force results for the different cases considered for the inner and outer shields during discharge. Figures 3a - 3e show the patterns of the eddy currents for each model. The peak vector of the density of the eddy currents is shown at the bottom of the page. In Table 2 the data for each shield consist of five lines.

The first line of Table 2 reproduces the data in Table 1 obtained for a model with electrically insulated panels and tubes of adjacent panels electrically interconnected (at point A in Fig. 2); the eddy currents are shown in Fig. 3a.

The data in the second line was obtained for a model assuming that the tubes are electrically disconnected (at point A, Fig. 2). Comparison shows that the energy and the peak power in the second line are 20-30 times lower than those in the first line. The differences in the results for the models with continuous and discontinuous tubes are primarily caused by the currents in the circumferential direction induced in the areas of the shields near the edges where the panels are interconnected by tubes, forming a closed circular path (compare the patterns of eddy currents on Figs. 3a and 3b).

The third line in Table 2 represents a case for electrically insulated panels without tubes. The Joule losses for this case are about 2/3 of the losses for the case of electrically insulated panels with discontinuous tubes.

The fourth and the fifth lines of Table 2 show an attempt to take into account the possible impact of the presence of the superinsulation.

Since the real structure of the superinsulation is too complicated to model, it was modeled as a cylinder (see Fig. 3d) with a cut along the Z-axis, a thickness of 0.002 mm (40 layers of superinsulation with thickness of 2*250 A), and a radius of the corresponding shield. The results for this model, presented in the fourth line of the table, show that the heating of the superinsulation is much less than that of the panel itself.

The model used for the fifth line is different from the one corresponding to the second line only in that for this case the panels are no longer electrically insulated; their edges are connected via a single layer of superinsulation (with thickness of $5*10^{-8}$ m, and resistivity of $5.6*10^{-8}$ ohm*m). In this case the superinsulation once again provides the eddy currents with a path in the circumferential direction (see Fig. 3e), which causes a substantial growth of the heat deposition. The maximum current density in the superinsulation in between the panels is about $1.04*10^{9}$ A/m^2, which is not feasible since this material cannot carry such a high current density. This result shows that to reduce the Joule heating of the shields the aluminized layer of the superinsulation must be prevented from shorting adjacent panels via an insulating layer.

At the bottom of Table 2, the data for the end panels are presented. They show that the heating and the forces in the end panels are small compared to those in the cylindrical panels. The patterns of eddy currents in one half of the left end panel are shown on Fig. 3f.

The Complex Model Analysis

So far the outer and the inner shields as well as the right and the left end panels have been studied separately. What follows shows the correspondence between the previous results and the results obtained for a model including all the panels of the radiation shields. This model is presented in Fig. 4a, where half of one of the 16 radiation shields, with symmetry with respect to the plane DCFG, is shown in the left hand part of the page. The halves of the individual panels, marked by the points in the corners, are shown in the right hand part of the page. The panels comprising this model can be electrically insulated from each other, in which case the model assumes the conditions of an insulated edge along lines AD, BC, EF, HG, and ABEH. The same mesh (shown in Fig. 4a) was used to model a case in which the panels were electrically connected to each other. In that case the conditions of the insulated edge were imposed only along ABEH.

Table 3 shows the comparison of the data for the case with panels electrically insulated from each other. The first four lines are obtained for the models, when the panels were considered individually as those in Table 2; the fifth line is the result of the summation of the heating energy during discharge, the power and the forces (at 2 s) in the panels, shown in the first four lines. The last line shows the data obtained for the model including all the panels (see Fig. 4a). The panels are marked as in Fig. 4a. These results yield the following conclusions. First, since the differences between the data of the fifth and the last lines are relatively small (the difference in Fx is not essential, since $|Fx| << |Fy|$), the results of the previous analyses are valid for the case. Second, the distributions among the panels of the total heating energy during discharge and the power at a given moment of time (2 s) are proportional to each other, which fact will be used in what follows.

Table 4 gives the comparison of the data obtained for the models shown in Fig.4a. The first set of data in Table 4 corresponds to the case in which the panels are electrically insulated from each other, the second set of data to the case in which the panels are electrically connected to each other. Since EDDYCUFF does not provide a reasonably simple way to output the distribution of the total energy deposition among the parts of the structure during the calculation time and of the forces acting on parts of the structure, some data are missing in this table. Nonetheless, the estimates for the distributions of the energy deposition among the panels are shown (*in italics*) based on the scaling by the distribution of the power obtained by EDDYCUFF. All the data necessary to obtain the forces on the parts of the structure are kept in the output files and are available if needed.

The conclusions based on Table 4 are as follows

* The model with the panels electrically connected to each other versus the model with the electrically insulated panels shows slightly higher (by about 20%) values of energy, power, and electromagnetic forces.

* The distributions of the Joule heating among the panels in the two cases are essentially different. In the case of electrically connected panels the energy generated in the right end panel accounts for 11.5% of the total energy in the structure, whereas in the case of electrically insulated panels it accounts for only 1.9%. This is caused by redistribution of the eddy currents in the structure. The patterns of the eddy currents for these two cases are shown on Fig. 4b (for the model with electrically insulated panels), and on Fig.4c (for the case of electrically connected panels). If it is necessary to reduce the heating of the right end panel, a cut along line CD is suggested.

---

1 EDDYCUFF User's Manual ... (To be published)

2 A.F.Clark, G.E.Childs, G.H.Wallace Electrical Resistivity of Some Engineering Alloys at Low Temperatures. Cryogenics. August 1970, pp. 295-305.

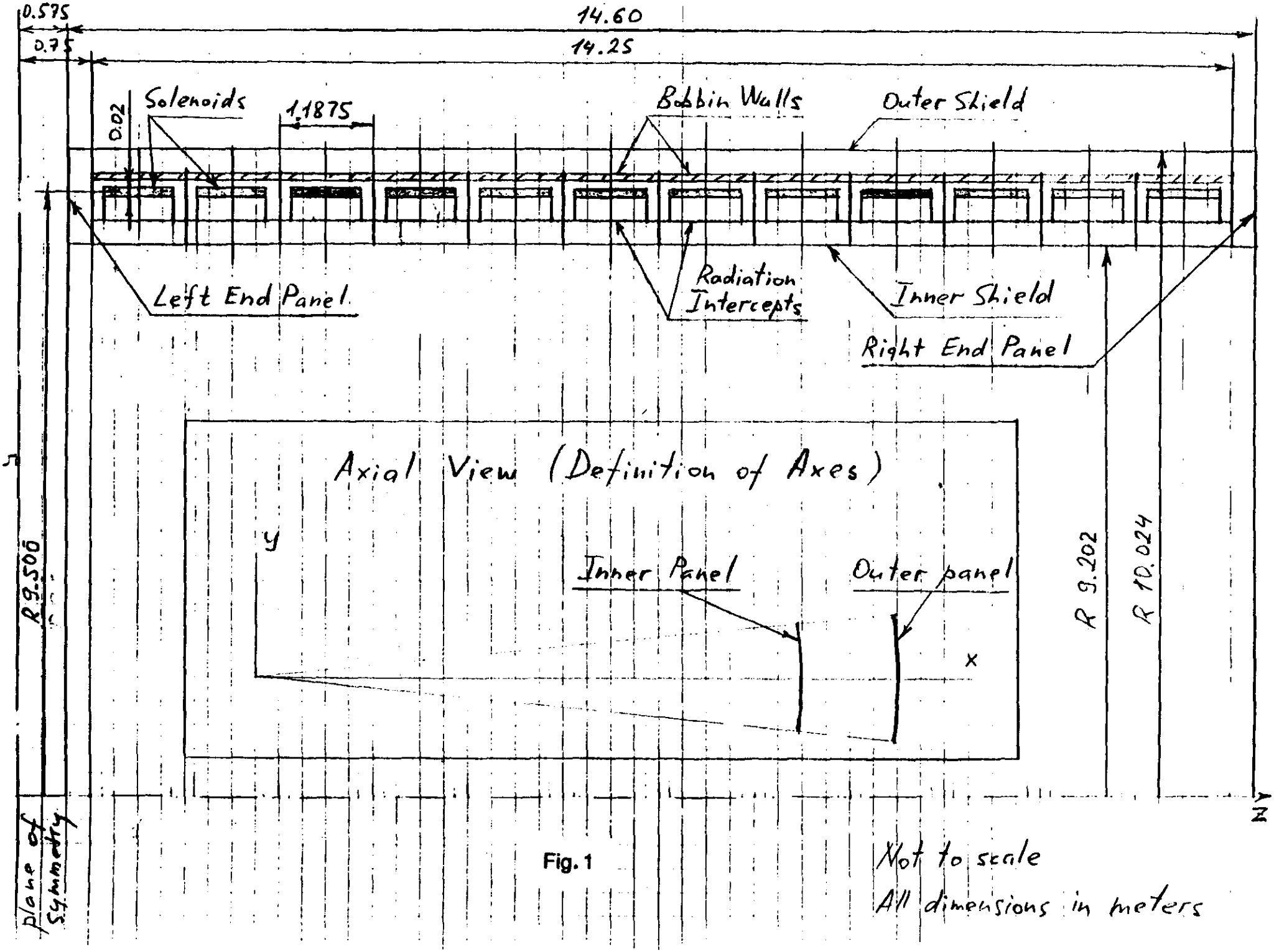
0.575
14.60
0.75
14.25
0.02
Solenoids
1.1875
Bobbin Walls
Outer Shield
Left End Panel
Radiation Intercepts
Inner Shield
Right End Panel
Axial View (Definition of Axes)
y
Inner Panel
Outer panel
x
R 9.506
R 9.202
R 10.024
Plane of Symmetry
Not to scale
All dimensions in meters

Fig. 1

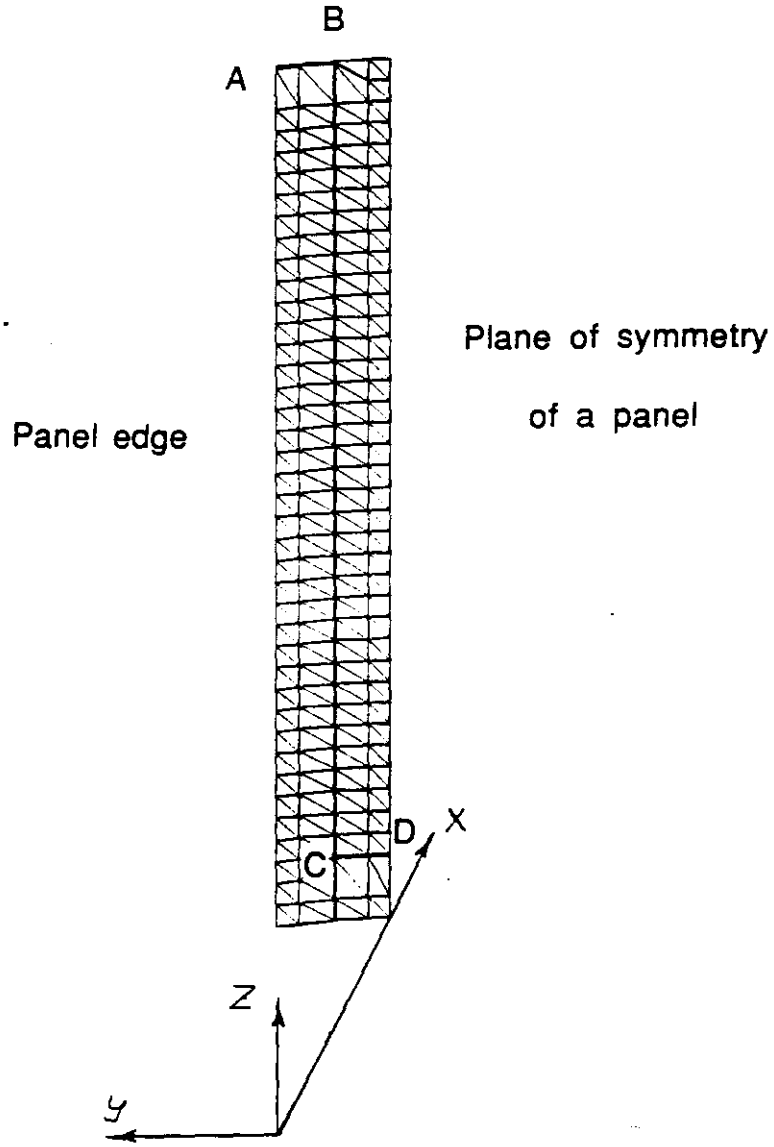

Fig. 2 Half of a Panel

With tubes							
		Energy and power in all 16 panels			Forces on a half of a panel		
Shield	Regime	Energy, J	Time	Power, W	Fx, N	Fy, N	Fz, N
Inner	Charge	4.462E+03	0-8 h	1.549E-01	-2.850E+01	-2.635E+01	2.210E+01
Outer	Charge	4.855E+03	0-8 h	1.686E-01	7.067E+00	-2.283E+01	2.147E+01
Inner	Discharge	6.478E+05	2 s	1.252E+04	8.018E+03	7.246E+03	-6.284E+03
Outer	Discharge	7.040E+05	2 s	1.360E+04	-1.949E+03	6.255E+03	-5.851E+03

Table 1 Comparison of Thermal Energy and Forces in Radiation Shields During Charge and Discharge

	Discharge								
	Inner Shield								
				Energy and power in all 16 panels			Forces on a half of a panel		
Line	Panels	Tubes	Superinsul.	Energy, J	Time	Power, W	Fx, N	Fy, N	Fz, N
1	Insulated	Continuous	Without	6.478E+05	2 s	1.252E+04	8.018E+03	7.246E+03	-6.284E+03
2	Insulated	Discont.	Without	2.313E+04	2 s	4.488E+02	2.127E+02	1.253E+03	3.983E+02
3	Insulated	Without	Without	1.612E+04	1 s	3.192E+02	1.538E+02	8.122E+02	2.850E+02
4	Without	Without	All	7.556E+01	1 s	1.505E+00	n/a	n/a	n/a
5	Conn.via superins.	Discont.	Conn.panels	4.026E+04	1 s	8.017E+02	4.448E+02	-2.822E+02	-1.910E+02
	Discharge								
	Outer Shield								
				Energy and power in all 16 panels			Forces on a half of a panel		
Line	Panels	Tubes	Superinsul.	Energy, J	Time	Power, W	Fx, N	Fy, N	Fz, N
1	Insulated	Continuous	Without	7.040E+05	2 s	1.360E+04	-1.949E+03	6.255E+03	-5.851E+03
2	Insulated	Discont.	Without	2.470E+04	2 s	4.792E+02	-2.810E+02	1.194E+03	3.912E+02
3	Insulated	Without	Without	1.759E+04	1 s	3.484E+02	-2.130E+02	8.021E+02	2.859E+02
4	Without	Without	All	7.684E+01	1 s	1.530E+00	n/a	n/a	n/a
5	Conn.via superins.	Discont.	Conn.panels	4.172E+04	2 s	8.308E+02	-7.121E+01	-2.797E+02	-1.970E+02
	Discharge								
	End panels			Energy and power in all 16 panels			Forces on a half of a panel		
				Energy, J	Time	Power, W	Fx, N	Fy, N	Fz, N
Left	Insulated			1.503E+02	1 s	2.993E+00	-2.413E+01	3.668E+00	-3.868E+00
Right	Insulated			6.220E+01	1 s	1.239E+00	-8.046E+00	1.694E+00	7.183E-01

Table 2 Summary of Thermal Energy and Forces in Radiation Shields

Fig.3a Distribution of Current Density During Discharge in One Half of the Outer Shield Panel with Azimuthally Continuous Tubes

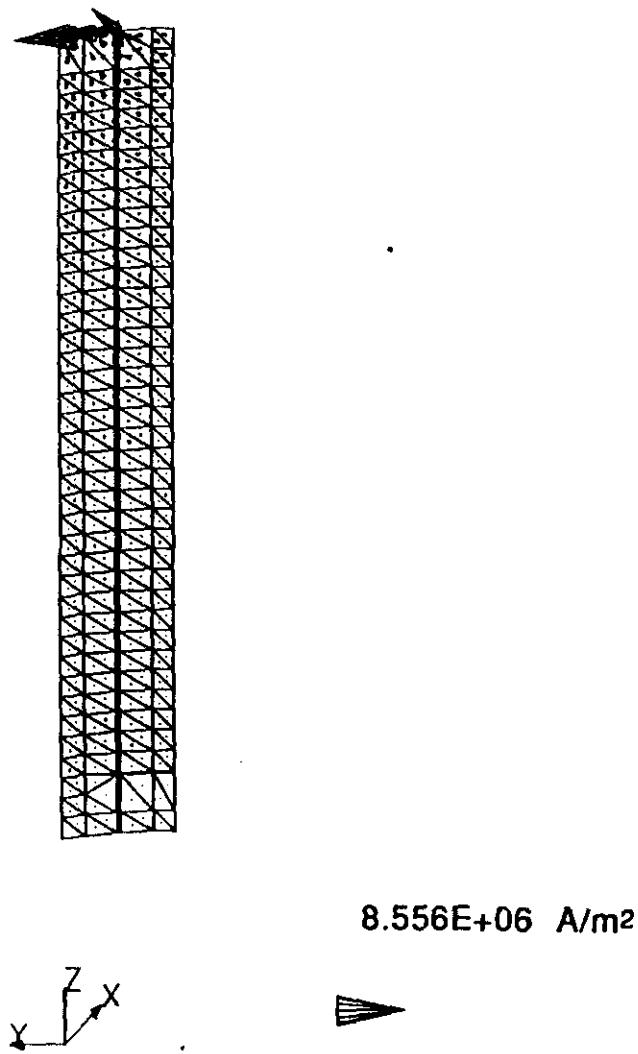

Fig.3b Distribution of Current Density During Discharge in One Half of the Outer Shield Panel with Azimuthally Discontinuous Tubes

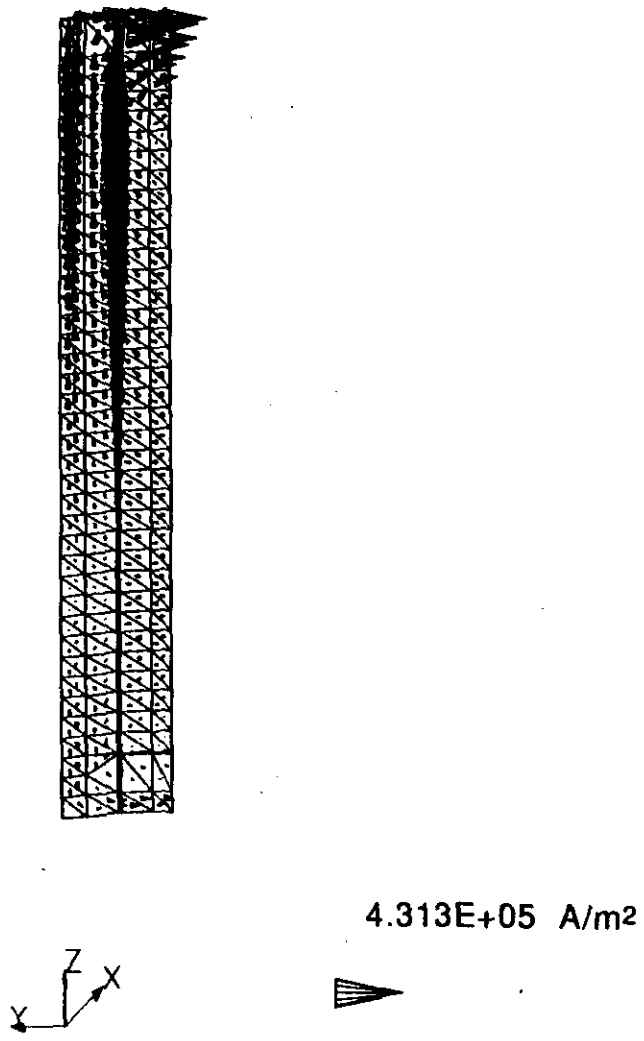

Fig.3c Distribution of Current Density During Discharge in One Half of the Outer Shield Panel without Tubes

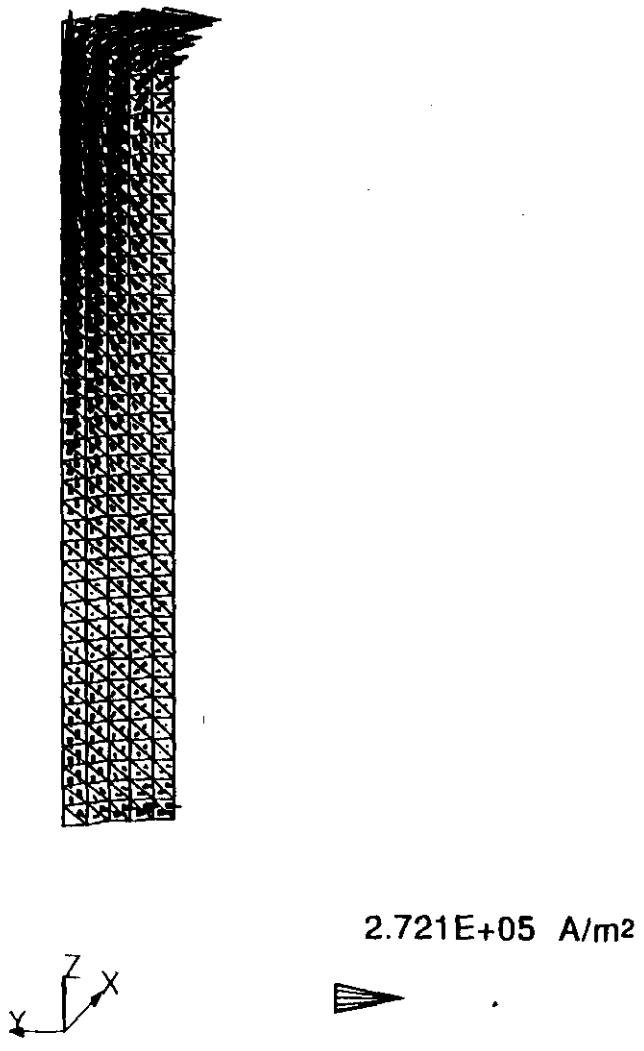

Fig.3d Distribution of Current Density During Discharge in the Superinsulation of the Outer Shield

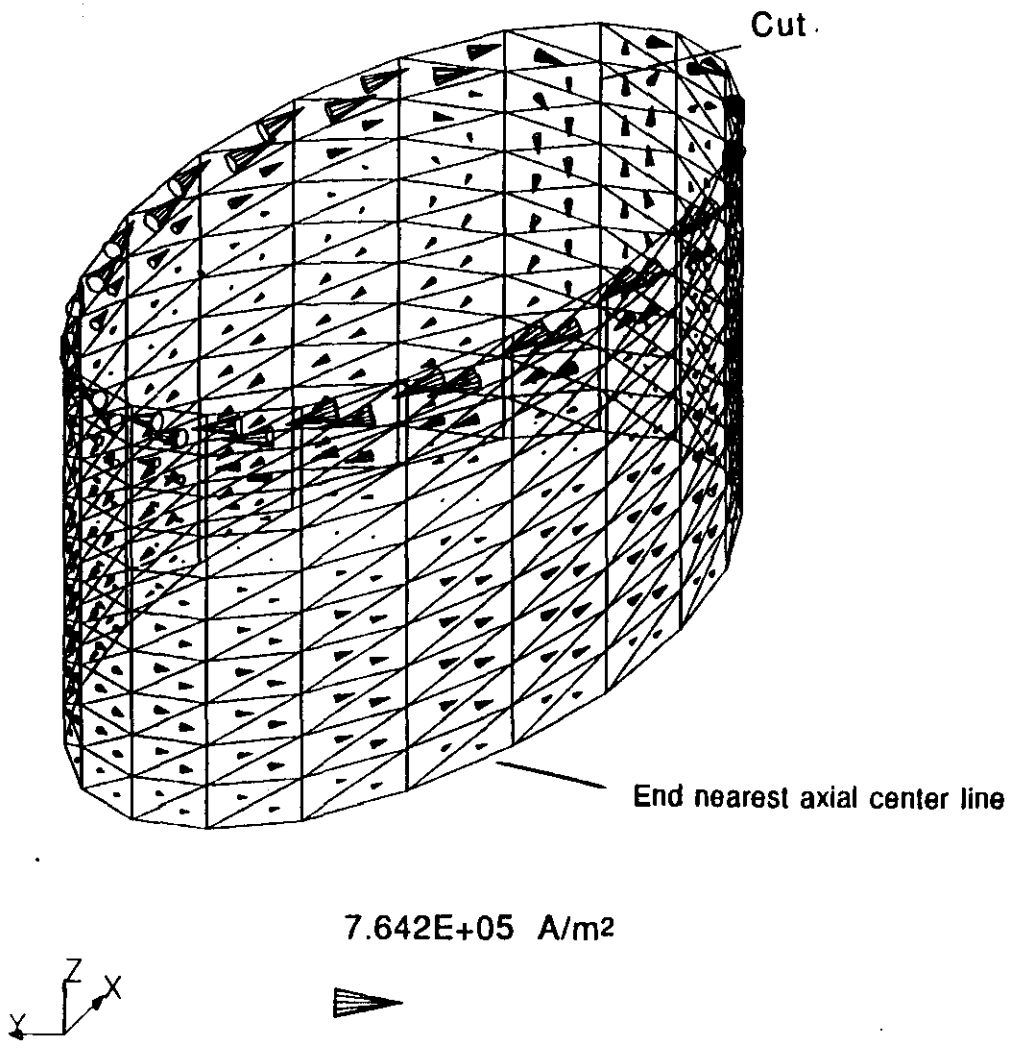

Fig.3e Distribution of Current Density During Discharge in One Half of the Outer Shield Panel when the Panels are Electrically Connected via the Superinsulation

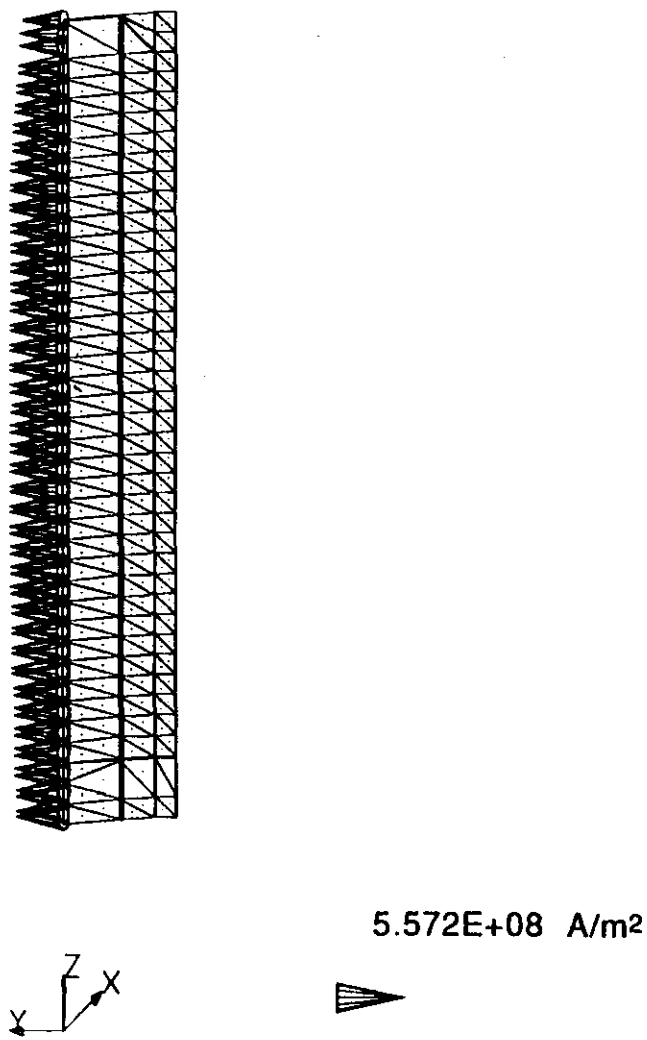

Fig.3f Distribution of Current Density During Discharge in One Half of the Left End Panel

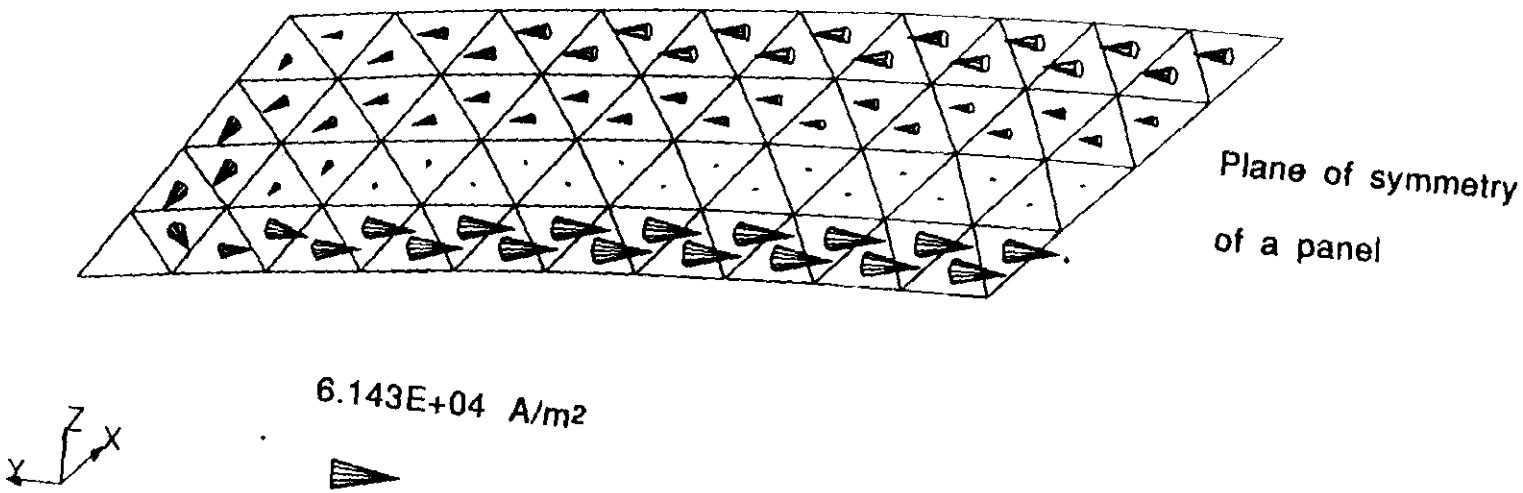

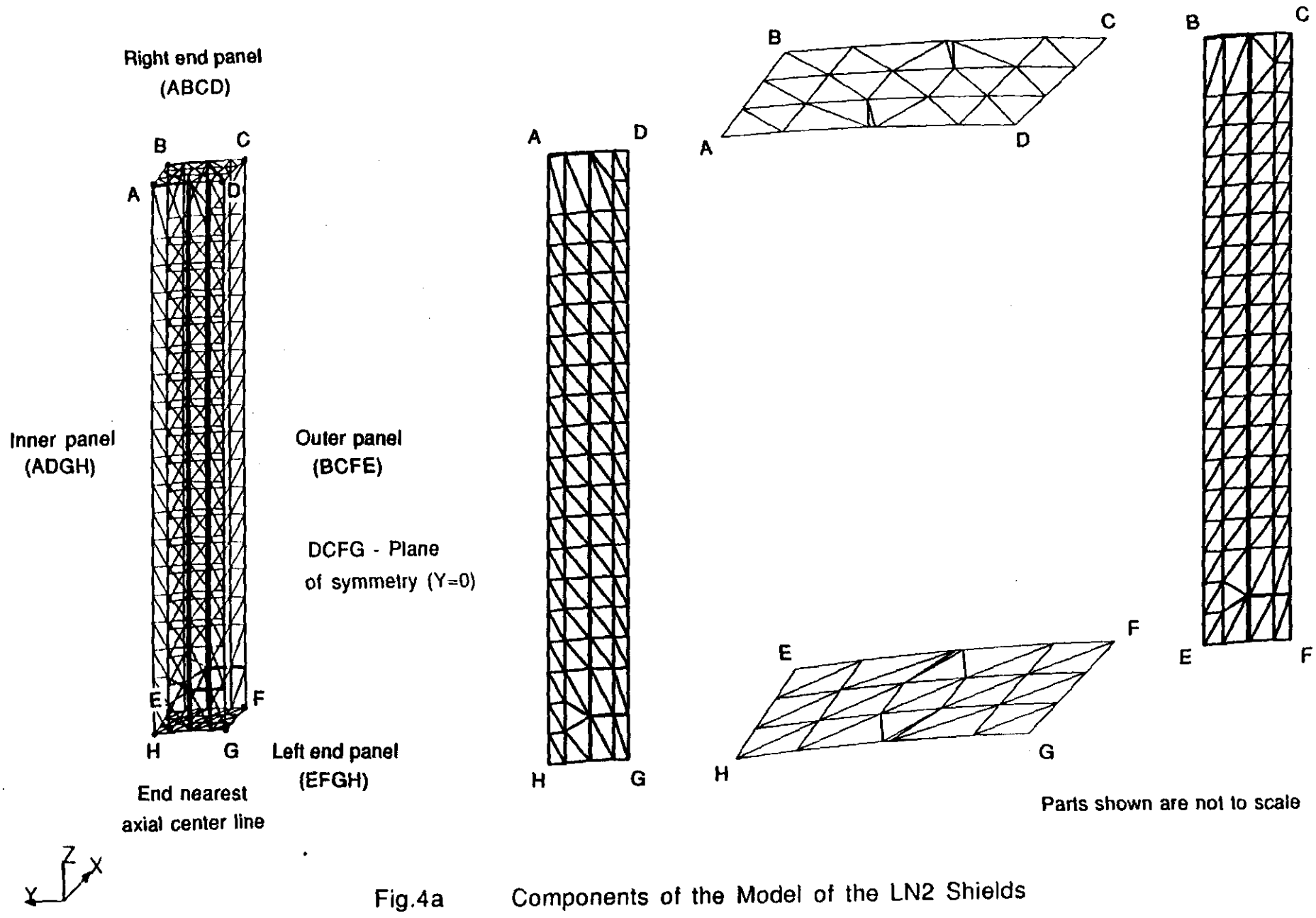

Fig.4a Components of the Model of the LN2 Shields

Discharge											
				Energy and power in all 16 panels					Forces on a half of a panel		
Panels	El.cond.	Tubes	Superins.	Energy, J	J, %	Time	Power, W	W, %	Fx, N	Fy, N	Fz, N
ADGH:Inner	Insulated	Discon.	Without	2.313E+04	48.145%	2 s	4.488E+02	48.147%	2.127E+02	1.253E+03	3.983E+02
BCFE:Outer	Insulated	Discon.	Without	2.470E+04	51.412%	2 s	4.792E+02	51.408%	-2.810E+02	1.194E+03	3.912E+02
EFGH:Left	Insulated	Without	Without	1.503E+02	0.313%	2 s	2.934E+00	0.315%	-2.365E+01	3.596E+00	-3.792E+00
ABCD:Right	Insulated	Without	Without	6.220E+01	0.129%	2 s	1.214E+00	0.130%	-7.887E+00	1.660E+00	7.040E-01
All 4 (sum.)	Insulated		Without	4.804E+04	100%		9.322E+02	100%	-9.984E+01	2.452E+03	7.864E+02
All 4 (calc.)	Insulated		Without	4.610E+04		2 s	8.990E+02		-6.636E+01	2.331E+03	7.349E+02

Table 3 Comparison of the Data for Individual Panels vs. the Entire Shield when the Panels Are Electrically Insulated

Discharge										
				Energy and power in all 16 panels				Forces on a half of a panel		
Panels	El.cond.	Tubes	Superinsul.	Energy, J	Time	Power, W	W,%	Fx, N	Fy, N	Fz, N
ADGH:Inner	Discon.	Discont.	Without	*2.233E+04*	2 s	4.354E+02	48.4%			
BCFE:Outer	Discon.	Discont.	Without	*2.276E+04*	2 s	4.438E+02	49.4%			
EFGH:Left	Discon.	Without	Without	*1.367E+02*	2 s	2.665E+00	0.3%			
ABCD:Right	Discon.	Without	Without	*8.843E+02*	2 s	1.724E+01	1.9%			
All 4 (calc.)	Discon.		Without	4.610E+04	2 s	8.990E+02	100.0%	-6.636E+01	2.331E+03	7.349E+02
ADGH:Inner	Contin.	Discont.	Without	*2.256E+04*	2 s	4.398E+02	40.8%			
BCFE:Outer	Contin.	Discont.	Without	*2.580E+04*	2 s	5.030E+02	46.6%			
EFGH:Left	Contin.	Without	Without	*6.091E+02*	2 s	1.188E+01	1.1%			
ABCD:Right	Contin.	Without	Without	*6.366E+03*	2 s	1.241E+02	11.5%			
All 4 (calc.)	Contin.		Without	5.533E+04	2 s	1.079E+03	100.0%	-4.161E+02	2.790E+03	8.417E+02

Table 4 Distribution of Energy among the Panels when They are either Electrically Insulated or Connected to Each Other

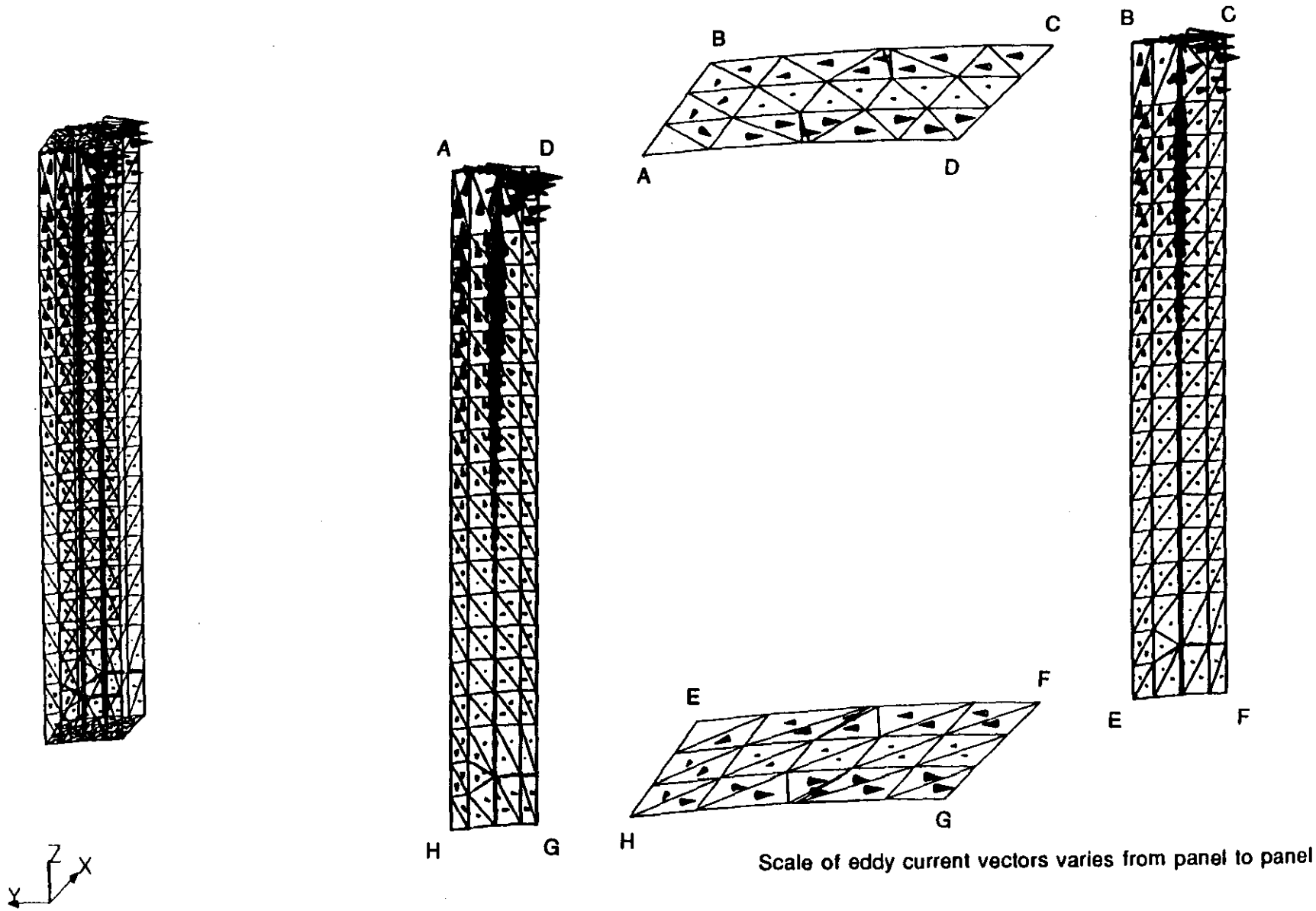

Fig.4b Eddy Currents in Individual Panels Electrically Insulated from Each Other

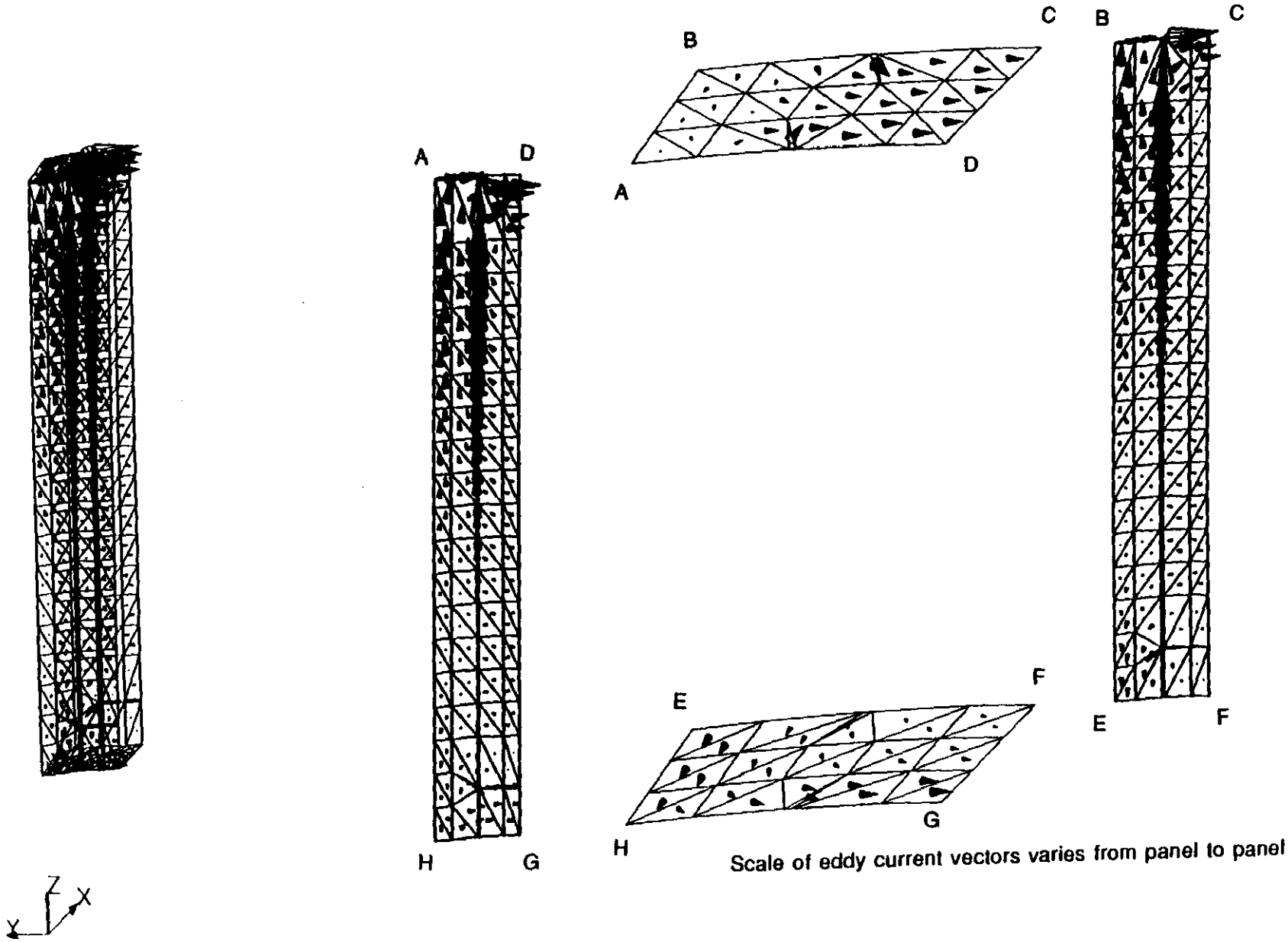

Fig. 4c Eddy Currents in Individual Panels Electrically Connected to Each Other